A&A 518, L93 (2010)
DOI: 10.1051/0004-6361/201014619

Herschel: the first science highlights

Astronomy & Astrophysics
Special feature

LETTER TO THE EDITOR

Galactic cold cores: *Herschel* study of first *Planck* detections⋆,⋆⋆

M. Juvela[1,2], I. Ristorcelli[3], L. A. Montier[3], D. J. Marshall[3], V.-M. Pelkonen[2,5], J. Malinen[1,2], N. Ysard[1,2], L. V. Tóth[6], J. Harju[1,2], J.-P. Bernard[3], N. Schneider[8], E. Verebélyi[6], L. Anderson[7], P. André[8], M. Giard[3], O. Krause[4], K. Lehtinen[1,2], J. Macias-Perez[12], P. Martin[10], P. M. McGehee[5], C. Meny[3], F. Motte[8], L. Pagani[9], R. Paladini[5], W. Reach[5], L. Valenziano[11], D. Ward-Thompson[12], and A. Zavagno[7]

1 Department of Physics, F00014, University of Helsinki, Finland
e-mail: mika.juvela@helsinki.fi
2 Observatory, University of Helsinki, Finland 1
3 CESR, Observatoire Midi-Pyrénées (CNRS-UPS), Université de Toulouse, BP 44346, 31028 Toulouse Cedex 04, France
4 Max-Planck-Institut für Astronomie, Königstuhl 17, 69117, Heidelberg, Germany
5 IPAC, Caltech, Pasadena
6 Loránd Eötvös University, Department of Astronomy, Pázmány P.s. 1/a, 1117 Budapest, Hungary (OTKA K62304)
7 Laboratoire d'Astrophysique de Marseille, 38 rue F. Joliot-Curie, 13388 Marseille Cedex 13, France
8 Laboratoire AIM, CEA/DSM - INSU/CNRS - Université Paris Diderot,IRFU/SAp CEA-Saclay, 91191 Gif-sur-Yvette, France
9 LERMA & UMR 8112 du CNRS, Observatoire de Paris, 61 Av. de l'Observatoire, 75014 Paris, France
10 University of Toronto, CITA, Canada
11 INAF/IASF, Bologna, Italy
12 LPSC, Université Joseph Fourier Grenoble I, CNRS/IN2P3, Institut National Polytechnique de Grenoble, 53 Avenue des Martyrs, 38026 Grenoble Cedex, France
13 School of Physics and Astronomy, Cardiff University, Cardiff, UK

Received 31 March 2010 / Accepted 20 April 2010

ABSTRACT

Context. We present the first results from the project Galactic cold cores, where the cold interstellar clouds detected by the *Planck* satellite are studied with *Herschel* photometric observations. The final *Planck* catalogue is expected to contain several thousand sources. The *Herschel* observations during the science demonstration phase provided the first glimpse into the nature of these sources.
Aims. The main goal of the project is to derive the physical properties of the cold core population revealed by *Planck*. We examine three fields and confirm the *Planck* detections with *Herschel* data, which we also use to establish the evolutionary stage of the identified cores.
Methods. We study the morphology and spectral energy distribution of the sources using the combined wavelength coverage of *Planck* and *Herschel*. The dust colour temperatures and emissivity indices are determined. The masses of the cores are determined with distance estimates which are taken from the literature and are confirmed by kinematic and extinction information.
Results. The observations reveal extended regions of cold dust with dust colour temperatures down to $T_{\rm dust} \sim 11$ K. The fields represent different evolutionary stages ranging from a quiescent, cold filament in Musca to regions of active star formation in Cepheus.
Conclusions. The *Herschel* observations confirm that the all-sky survey of *Planck* is capable of making a large number of new cold core detections. Our results suggest that many of the sources may already have left the pre-stellar phase or are at least closely associated with active star formation. High-resolution *Herschel* observations are needed to establish the true nature of the *Planck* detections.

Key words. ISM: clouds – infrared: ISM – submillimeter: ISM – dust, extinction – stars: formation – stars: protostars

1. Introduction

A key question in the study of star formation is which force forms the cloud cores, whose gravitational collapse leads to the birth of new stars. Interstellar clouds have a complex structure whose origin can be traced to the properties of turbulence (e.g., Padoan et al. 2004; de Avillez & Breitschwerdt 2007; Schneider et al. 2010). At scales of several parsecs, gravitation has a minor effect on the general density field (see, however, Goodman et al. 2009). At small scales the roles are reversed as the development of protostellar systems is dictated by gravitation, still resisted by turbulent and kinetic pressures and feedback from forming stars (Zinnecker & Yorke 2007). Between these two scales the situation is less clear. Turbulent motions, gravitational fragmentation, and external triggering all contribute to the formation of the pre-stellar cores (Bergin & Tafalla 2007; McKee & Ostriker 2007; Ward-Thompson et al. 2007). Which is the dominant process, and does the situation vary from region to region? The magnetic field is another poorly constrained factor (Crutcher et al. 2009).

⋆ *Planck* (http://www.esa.int/Planck) is a project of the European Space Agency – ESA – with instruments provided by two scientific consortia funded by ESA member states (in particular the lead countries: France and Italy) with contributions from NASA (USA), and telescope reflectors provided in a collaboration between ESA and a scientific Consortium led and funded by Denmark.

⋆⋆ *Herschel* is an ESA space observatory with science instruments provided by European-led Principal Investigator consortia and with important participation from NASA.

Table 1. The observed fields.

Target	RA (J2000)	Dec (J2000)	Map size (PACS/SPIRE)
PCC 249	22 21 17.6	+63 42 25	50′/50′
PCC 288	22 53 31.3	+62 31 44	18′/30′
PCC 550	12 25 16.5	−71 46 03	18′/30′

Is star formation regulated or only slightly modified by the magnetic field?

To answer these questions we need to study many cores that cover the transition from large scale density field to protostellar systems. We are faced with two partly contradictory requirements. We need not only a sample representative of the full range of masses, environments, and evolutionary stages, but also high-resolution data to resolve the structures that could give information on the core formation mechanisms. In pre-stellar cores most molecules can be frozen out of the gas phase. Because of the low temperature dust emission is weak even in the far-infrared, and studies must be carried out at sub-millimetre wavelengths.

Planck and *Herschel* provide the complementarity needed for a study of a representative cross section of the Galactic cold core population. Thanks to its sensitivity, wide wavelength coverage, and a spatial resolution comparable with IRAS, the *Planck* all-sky survey is ideal for the target selection. In the *Herschel* open time key program Galactic cold cores, some 150 target fields will be mapped with the *Herschel* PACS and SPIRE instruments. We present the first results of this survey using data on three fields observed in the *Herschel* science demonstration phase (SDP). The paper concentrates on compact sources, their spectral energy distributions, and evolutionary stages.

2. Observations

Planck is performing an all-sky survey at nine wavelengths between 350 μm and 1 cm (Tauber et al. 2010). In August 2009, *Planck* completed the First Light Survey (FLS), which covers a band of about 15 degrees, mainly at low and middle Galactic latitudes. With the methods described in Montier et al. (2010), a catalogue of cold cores was created. Three fields were selected for SDP observations (see Table 1). The selection criteria were a high significance of the *Planck* detection of the cold dust signature, low colour temperature ($T < 14$ K using *Planck* and IRAS 100 μm data), and good visibility during SDP. Areas covered by other *Herschel* guaranteed time programmes were excluded.

The *Herschel* observations were conducted in November and December 2009. The field PCC 249 was observed in parallel mode, while the other observations were made with normal scan mapping, one instrument at a time. All SPIRE observations (250, 350, 500 μm) were made with two orthogonal scanning directions. In the fields PCC 249 and PCC 550, a similar observing strategy was used for PACS (100 and 160 μm). In PCC 288 we used three scanning directions which were 45 degrees apart. For details about *Herschel* and its instruments, see Pilbratt et al. (2010), Poglitsch et al. (2010), and Griffin et al. (2010). The data were reduced with the *Herschel* interactive processing environment (HIPE) v.2, using the official pipeline and e.g. masking of source regions during the fit of scan baselines. The PACS maps were created using the madmap algorithm. The SPIRE maps are the product of direct projection onto the sky and averaging of the time ordered data. We use the *Planck* internal data release v.3.1.

Parts of the PCC288 and PCC249 fields were mapped in January 2010 with the Onsala 20 m radio telescope in ^{13}CO and C^{18}O J = 1–0 lines. Additional ^{12}CO spectra were measured towards selected sub-mm peaks. The same regions were observed in NH_3 (1,1) and (2,2) lines with the Effelsberg 100 m radio telescope between November 2009 and January 2010. In both observations the FWHM of the antenna is about 40″. The obtained line parameters and the gas kinetic temperatures as derived from the ammonia observations are listed in Table 3. A detailed description of these data will be given in forthcoming papers.

3. Results

3.1. Field PCC288

In PCC288, the *Planck* detection of cold dust coincides with a group of sources (see Fig. 1). Our field is located west of the H II region Sh 2-155 (Sharpless 1959) and is illuminated by stars of the Cep OB3b group which, with an estimated age of 5.5 Myr (Jordi et al. 1996) and a distance of 600–900 pc (Reipurth et al. 2007), is one of the youngest nearby stellar groups. The south edge of our field corresponds to the centre of the cloud Cep F in Sargent et al. (1977) which, based on radial velocities, is associated with the OB group. Our line observations and the extinction of stars as a function of distance (for the method, see Marshall et al. 2009) suggest that the *Planck* source belongs to the same cloud. The clump *B* (see Fig. 1) hosts FU Ori-type star V733Cep, which is associated with an outflow (Reipurth et al. 2007) also visible in our ^{13}CO data. This is direct evidence of starformation which may have been triggered by the OB association. Some stars of the OB3a subgroup are inside our field.

To measure source spectra, we convolved observations to the SPIRE 500 μm resolution and used values in an aperture of 73″(twice the FWHM at 500 μm). Another set of spectra was determined using a 36″aperture and 100–250 μm data at the 250 μm resolution, 18″. Finally, for a comparison with the *Planck* data, fluxes were derived with a 9′ aperture and data convolved to a 4.5′ resolution. Aperture photometry was performed subtracting background in an annulus that extends 1.3–1.8 times that of the aperture radius. No aperture correction was done, but for a point source, it would be equal ~7%. Because the annulus may contain signal from other sources, the background was estimated using a 30% percentile instead of a mean. Especially for bright sources, the noise is small compared to the surface brightness fluctuations. Therefore the flux uncertainty was estimated with the interquartile interval divided by the square root of the number of resolution elements in the annulus.

The aperture positions are shown in Fig. 1. In addition to the three compact sources in the middle of the field PCC288, two more diffuse areas were included. The source *D* becomes visible only at SPIRE wavelengths, while the source *E*, an elongated structure NE of the field centre, is prominent in PACS bands. The flux estimates and the results of the greybody fits are given in Table 2. The data were iteratively colour-corrected using the fitted spectra. With the intensity and temperature obtained from the fit, a distance of 800 pc, and dust κ_{850} = 0.02 cm^2 g^{-1} (see, e.g., Nutter et al. 2006 and references therein), we obtained an estimate of 140 solar masses for the 9′ aperture. For the brightest core *A*, the estimated mass is ~8.6 $M_\odot$ within the 73″aperture. The density profiles of cores *A* and *B* are shown in Fig. 2.

3.2. Field PCC550

The field PCC550 is located in Musca and contains a single cold filament. The *Herschel* maps reveal two distinct far-infrared peaks, which are also found in the IRAS point source catalogue (100 μm detections only) and the dark cloud catalogue of Dobashi et al. (2005). The cores were observed in the ^{13}CO and

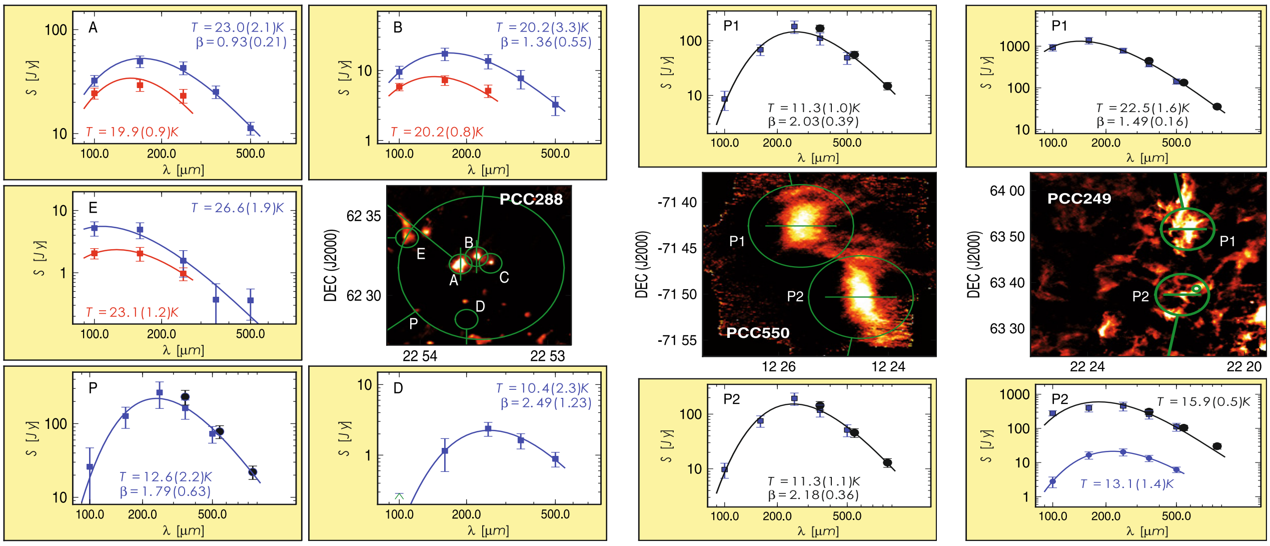

Fig. 1. Spectral energy distributions of selected areas in PCC288 (*left*), PCC550 (*middle*), and PCC249 (*right*). The maps show the PACS 100 μm (PCC288 and PCC249) or 160 μm (PCC550) intensity. For PCC288, greybody fits are presented for 100–500 μm data using 73″apertures (blue squares and lines; the smaller circles on the map) and for 110–250 μm data using 36″apertures (red squares and lines). For PCC288-P and the areas in PCC550 and PCC249, the fits employ 9′ apertures and include the *Planck* fluxes (black circles). If the value of β is not quoted, a fixed value of β = 2.0 was assumed. The vertical and horizontal lines indicate the cuts used in Fig. 2. The source coordinates are given in Table 2.

Table 2. The measured fluxes and parameters of fitted greybody spectra ($T_{\rm dust}$, β).

Area	RA (J2000)	Dec (J2000)	Fluxes [Jy] 100 μm	160 μm	250 μm	350 μm	500 μm	$T_{\rm dust}$ [K]	β
PCC288-A	22 53 41.0	+62 31 58	32.4(3.9)	49.4(6.4)	42.8(6.1)	25.2(3.5)	11.2(1.6)	23.0(2.1)	0.93(0.21)
PCC288-B	22 53 33.5	+62 32 26	9.5(2.0)	17.3(3.5)	13.7(3.2)	7.7(2.3)	3.2(1.0)	20.2(3.3)	1.36(0.55)
PCC288-C	22 53 26.9	+62 32 1	4.6(1.3)	8.9(3.7)	7.2(3.4)	4.2(2.4)	1.7(1.0)	19.6(3.5)	1.39(0.82)
PCC288-D	22 53 38.2	+62 28 30	–0.0(0.3)	1.1(0.6)	2.4(0.5)	1.6(0.4)	0.9(0.2)	10.4(2.3)	2.49(1.23)
PCC288-E	22 54 6.2	+62 33 37	5.2(1.4)	4.9(1.4)	1.6(0.7)	0.4(0.3)	0.4(0.2)	26.6(1.9)	2.0 (fixed)
PCC288-P	22 53 31.3	+62 31 44	25.9(20.9)	127(41)	265(104)	162(48)	72.8(18.5)	12.6(2.2)	1.79(0.63)
PCC550-P1	12 25 35.6	–71 42 35	9.2(3.5)	67.5(14.9)	180(46)	110(28)	49.1(12.1)	11.3(1.0)	2.03(0.39)
PCC550-P2	12 24 30.0	–71 50 19	8.9(2.7)	74.9(17.8)	196(50)	118(29)	51.1(12.7)	11.3(1.1)	2.18(0.36)
PCC249-P1	22 21 26.7	+63 51 37	1016(184)	1329(242)	761(105)	365(51)	143(21)	22.5(1.6)	1.49(0.16)
PCC249-P2	22 21 35.0	+63 37 22	304(53)	387(91)	447(130)	257(70)	113(30)	15.9(0.5)	2.0 (fixed)

Notes. An aperture size of 73″ is used for PCC288 sources *A*–*E*. Otherwise, the aperture is 9′ and the fits include *Planck* fluxes at 857, 545, and 353 GHz (not listed; see Fig. 1).

$C^{18}O$ by Vilas-Boas et al. (1994). In their paper, our areas P1 and P2 (see Fig. 1) correspond to sources Mu5 and Mu4 with estimated masses of 32.9 $M_{\odot}$ and 16.5 $M_{\odot}$ (assuming d = 225 pc). The observed line widths of ~0.8 km s^{-1} and the derived excitation temperature of $T_{\rm ex}$ = 8 K are consistent with cold, quiescent cloud cores. Figure 1 shows the spectra of the two clumps averaged over 9′ apertures. The far-infrared data show no indication of warm sources and the density profiles are consistent with hydrostatic equilibrium (see Fig. 2). This suggests that the sources are potential pre-stellar cores. The whole filament is very cold, and the derived colour temperatures are ~11 K for the two cores. At a distance of 225 pc, the presented fits correspond to core masses of 9.2 $M_{\odot}$ and 8.1 $M_{\odot}$ for P1 and P2, respectively.

3.3. Field PCC249

Field PCC249 is an active region within the L1204/S140 complex just north of S140-IRS. The source S140-IRS is visible at the south edge of our SPIRE map, but falls just outside the PACS maps because of the pointing difference of the two instruments which affects maps made in parallel mode. The distance of S140 is ~1.3 kpc (Crampton & Fisher 1974).

Planck observations pointed to cold emission in two regions (large circles in Fig. 1). The area *P1* corresponds to the core G in the CS(1-0) mapping of Tafalla et al. (1993). The strongest emission is associated with the young stellar object IRAS 22198+6336, where both water masers and an outflow have been detected (Palla et al. 1991; Zhang et al. 2005). Using VLBI astrometry of H_2O maser spots, Hirota et al. (2008) obtained a distance estimate of 764 ± 27 pc similar to our extinction distance estimate of 900 pc. They concluded that the source is an intermediate mass YSO, still deeply embedded in a dense dust core. On the basis of ^{13}CO(2-1) observations, Wang et al. (2009) estimated a mass of ~1700 $M_{\odot}$ for the surrounding ~8′-diameter cloud, however, adopting a distance of 1.67 kpc. The second *Planck* detection (region P2) coincides with the Tafalla et al. core F. The area, also known as S140NE, contains small reflection nebulae and two Herbig-Haro objects (Bally et al. 2002).

According to the SEDs of Fig. 1 the estimated masses are 90 and 93 solar masses for regions P1 and P2, respectively (d = 800 pc). On the basis of *Planck* and IRAS data, P2 was a more secure detection of cold emission than P1. With a temperature of ~23 K, P1 no longer qualifies as a bona fide cold core. For P2, the derived temperature is lower, ~16 K for a fixed

Table 3. The ^{13}CO(1-0) and NH_3(1,1) line parameters and the the kinetic temperatures derived from the ammonia (1,1) and (2,2) lines.

Area	$T_A(^{13}CO)$ [K]	$v(^{13}CO)$ [km s^{-1}]	$\Delta v(^{13}CO)$ [km s^{-1}]	$T_A(NH_3)$ [K]	$v(NH_3)$ [km s^{-1}]	$\Delta v(NH_3)$ [km s^{-1}]	T_{kin} [K]
PCC288-A	2.89(0.03)	−9.18(0.01)	1.90(0.03)	2.00(0.03)	−9.041(0.002)	0.788(0.005)	13.4(0.2)
PCC288-B	2.61(0.04)	−9.35(0.01)	2.14(0.04)	0.83(0.03)	−9.037(0.004)	0.460(0.011)	10.9(0.7)
PCC249-P1	4.16(0.03)	−10.73(0.01)	2.63(0.03)	1.84(0.03)	−11.081(0.003)	1.264(0.007)	15.3(0.2)
PCC249-P2	4.21(0.03)	−10.21(0.01)	1.72(0.02)	1.94(0.03)	−10.835(0.003)	0.902(0.007)	14.3(0.3)

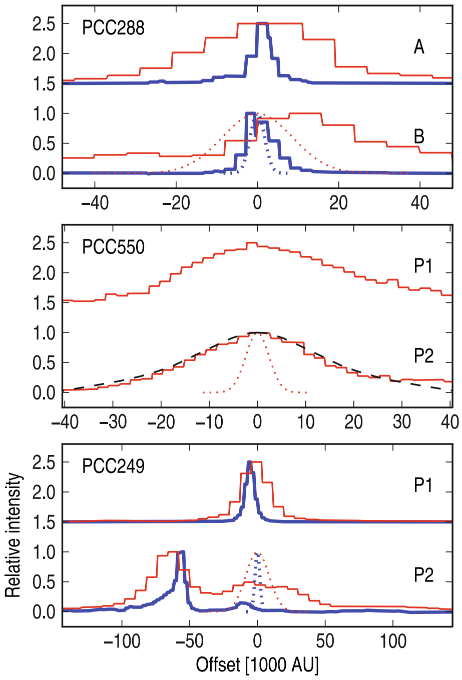

Fig. 2. Intensity profiles at 100 μm (thick blue lines) and 350 μm (thin red lines) across selected cores along the cuts shown in Fig. 1. The dotted lines indicate beam sizes. Positive offsets correspond to positions west or north of the reference position (see Table 2). For PCC550, the dashed line shows the column density profile of a Bonnor-Ebert sphere (Bonnor 1956; T = 11 K, ξ = 6.99, P_{ext} = 10^4 K cm^{-3}) without beam convolution. Each curve has been normalized with its peak value.

value of β = 2.0, and the shape of the SED hints at two temperature components. Despite the warm average temperatures, the apertures do contain some cold dust. The 73″ diameter circle marked in Fig. 1 inside the P2 area delineates one structure with an estimated temperature of ∼13 K (β = 2.0).

4. Conclusions

A number of compact dust clouds have been detected in the *Planck* First Light Survey. *Herschel* enables the determination of their SEDs and source morphologies at high resolution. In two fields selected for *Herschel* SDP observations, the *Herschel* data confirm the detections. In the third one, PCC249, the *Planck* sources correspond to dense clouds – but with a higher average colour temperature. The warm objects (as traced by the 100 μm data) are usually only marginally resolved, while the colder dust emission detected with SPIRE is always more extended. In PCC550 and PCC249, the cores are clearly part of a larger filamentary cloud structure.

The fields represent different phases of star formation. The field PCC550 is a cold, quiescent filament where the two submillimetre peaks are potential sites of future low-mass star formation. The field PCC288 contains a more massive and mainly cold dust cloud which however already contains young stellar objects that have raised the temperature of their environment. The average temperature over an aperture of 9′ is only 12.6 K. This shows that the warm sources are embedded in a colder envelope, which also is directly visible at SPIRE wavelengths. The location of PCC288 at the interface between the young Cep OB group towards north/east and molecular clouds towards south strongly suggests a scenario of sequential, triggered star formation. The third field, PCC249, is even more active, and this is reflected in the detection of extended regions of heated dust. Nevertheless, the field contains some colder areas with colour temperatures down to at least ∼13 K, i.e., potential pre-stellar cores. In PCC249 and PCC550, the derived core masses are smaller than the values previously derived from line data. This may be explained by the uncertainties of mass determination (e.g., the assumed value of κ) and the background subtraction that was not included in the analysis of line data. Nevertheless, the differences warrant further investigation.

The *Planck* detections are based on the residual cold emission after the warm component traced by 100 μm IRAS data is subtracted (Montier et al. 2010). The results of PCC249 suggest that in regions with large temperature variations the procedure can result in the detection of some sources of higher average temperature. However, the detection of colder sub-regions shows that even such active star-forming clouds can still be associated with significant amounts of cold dust. The diffuse dust component will be studied in more detail in following papers.

References

deAvillez, M., & Breitschwerdt, D. 2007, ApJ, 665, L35
Bally, J., Reipurth, B., Walawender, J., & Armond, T. 2002, AJ, 124, 2152
Bergin, E. A., & Tafalla, M. 2007, ARA&A, 45, 339
Bonnor, W. B. 1956, MNRAS, 116, 351
Crampton, D., & Fisher, W. A. 1974, Pub. Dom. Astrophys. Obs., 4, 283
Crutcher, R. M., Hakobian, N., & Troland, T. H. 2009, ApJ, 692, 844
Dobashi, K., Uehara, H., Kandori, R., et al. 2005, PASJ, 57, S1
Goodman, A., Rosolowsky, E. W., Borkin, M. A., et al. 2009, Nature, 457, 63
Griffin, M. J., et al. 2010, A&A, 518, L3
Hirota, T., Ando, K., Bushimata, T., et al. 2008, PASJ, 60, 961
Jordi, C., Trullols, E., & Galadi-Enriquez, D. 1996, A&A, 312, 499
Marshall, D. J., Joncas, G., & Jones, A. P. 2009, ApJ, 706, 727
McKee, C. F., & Ostriker, E. C. 2007, ARA&A, 45, 565
Montier, L., Pelkonen, V.-M., Juvela, M., et al. 2010, A&A, accepted
Nutter, D., Ward-Thompson, D., & André, P. 2006, MNRAS, 368, 1833
Padoan, P., et al. 2004, Phys. Rev. Lett., 92, 1102
Palla, F., et al. 1991, A&A, 246, 249
Pilbratt, G. L., et al. 2010, A&A, 518, L1
Poglitsch, A., et al. 2010, A&A, 518, L2
Reipurth, B., Aspin, C., Beck, T., et al. 2007, AJ, 133 1000
Sargent, A. I. 1977, ApJ, 218, 736
Sharpless, S. 1959, ApJS, 4, 257
Schneider, N., Bontemps, S., Simon, R., et al. 2010, A&A, submitted
Tafalla, M., Bachiller, R., & Martń-Pintado, J. 1993, ApJ, 403, 175
Tauber, J., Mandolesi, N., Puget, J.-L., et al. 2010, A&A, accepted
Vilas-Boas, J. W. S., Myers, P. C., & Fuller, G. A. 1993, ApJ, 433, 96
Ward-Thompson, D., André, P., Crutcher, R., et al. 2007, in Protostars and Planets V, ed. B. Reipurth, D. Jewitt, & K. Keil, 33
Wang, K., Wu, Y. F., Ran, L., Yu, W. T., & Miller, M. 2009, A&A, 507, 369
Zhang, Q., Hunter, T. R., & Brand, J. 2005, ApJ, 625, 864
Zinnecker, H., & Yorke, H. W. 2007, ARA&A, 45, 481